

Mean field heat transfer scaling for non-Newtonian stagnant lid convection

C.C. Reese^{a,*}, V.S. Solomatov^b

^a *Division of Science and Mathematics, University of Minnesota Morris, Morris, MN 56267, USA*

^b *Department of Physics, New Mexico State University, Las Cruces, NM 88003, USA*

Received 30 January 2002; received in revised form 9 July 2002

Abstract

Convection with asymptotically large viscosity contrasts occurs in the stagnant lid regime characterized by the formation of an immobile lid on top of a convective layer. Convection beneath the lid is driven by the rheological temperature scale rather than the entire temperature drop across the layer. A boundary layer treatment of the mean field hydrodynamic equations with infinite Prandtl number, no-slip boundary conditions, and temperature- and stress-dependent viscosity yields a scaling relationship for the stagnant lid heat flux. When the wavenumber is chosen such that the heat flux is maximized, the scaling relationship is in reasonable agreement with results of time-dependent, two-dimensional, convection simulations and boundary layer stability analysis. The best agreement with data occurs for pseudo-steady state, low Rayleigh number convection before the fully time-dependent asymptotic regime is reached.

© 2002 Elsevier Science B.V. All rights reserved.

Keywords: Thermoviscous convection; Heat transfer scaling; Boundary layer theory

1. Introduction

1.1. Stagnant lid convection

Thermal convection of a high Prandtl number fluid layer with temperature- and stress-dependent viscosity occurs in an asymptotic, stagnant lid regime for an effective viscosity contrast across the layer of $\geq 10^5$. In this regime, the most viscous part of the cold thermal boundary layer is rigid and only a thin sublayer at the bottom of the stagnant lid participates in convection. Stagnant lid convection was predicted by Newtonian boundary layer analyses [1,2], observed in laboratory experiments [3], and studied in numerical simulations [4–7]. Various numerical and experimental data were reconciled by the scaling

* Corresponding author.

E-mail address: resec@cda.mrs.umn.edu (C.C. Reese).

theory of [8]. Recently, the Newtonian boundary layer theories [1,2] were extended to non-Newtonian viscosity [9].

For Newtonian stagnant lid convection, heat transfer scaling laws obtained from boundary layer analyses [1,2] agree well with numerical simulations of steady convection [4,6]. Likewise, an extension of the boundary layer approach to the non-Newtonian case [9] showed approximate agreement with steady-state numerical studies [9,7]. Time-dependent Newtonian and non-Newtonian stagnant lid convection [6,7,10,11] are consistent with scaling relationships suggested by boundary layer stability and viscous dissipation analyses [8].

The purpose of this study is to suggest a heat transfer scaling for non-Newtonian stagnant lid convection based on a mean field approach. The advantage of this approximation is that limiting the flow in the lateral direction to a single spectral mode results in a simplified form of the hydrodynamic equations while retaining the strongest non-linear effect arising from modification of the horizontally averaged temperature distribution by the convective heat transfer. Furthermore, the single mode wavenumber which maximizes the heat transport is determined. The results are compared to previously suggested scalings and numerical simulations.

1.2. Viscosity

As in previous studies of stagnant lid convection, an exponential viscosity law is considered,

$$\eta = b\tau^{1-n} \exp(-\gamma T), \quad (1)$$

where b , n , and γ are constants, τ is the second invariant of the deviatoric stress tensor, and T is the temperature.

1.3. Non-dimensional parameters

The problem involves two non-dimensional parameters: the log viscosity contrast due to temperature alone:

$$\theta = \ln(\Delta\eta) = \gamma \Delta T, \quad (2)$$

and the Rayleigh number based on the interior temperature

$$Ra = \frac{\alpha \rho g \Delta T d^{(n+2)/n}}{b^{1/n} \kappa^{1/n} \exp(-\gamma T_i/n)}, \quad (3)$$

where α is the thermal expansivity, ρ is the density, g is the gravitational acceleration, ΔT is the temperature difference across the layer, d is the layer depth, κ is the thermal diffusivity and T_i is the interior temperature. The Nusselt number, Nu , is the average convective heat flux at the top of the lid normalized to the conductive heat flux across the layer for the same temperature difference.

1.4. Previous heat transfer scaling relationships

All stagnant lid Nusselt number scaling relations are of the form

$$Nu = A\theta^{-\zeta} Ra^\beta. \quad (4)$$

Boundary layer analyses [2,9] suggest that for lid thickness variations on the order of the lid thickness itself $A = 4.33$, $\zeta = 1$ and $\beta = n/(2n + 3)$. For small lid thickness variations [1,9], $A = 2.08$, $\zeta = 1 + \beta$ and $\beta = n/(2n + 3)$. Numerical simulations of stagnant lid convection indicate that while lid thickness variations are large for Newtonian viscosity [4], the lid is essentially flat for non-Newtonian ($n = 3$) viscosity [5].

In the non-Newtonian ($n = 3$) case, numerical experiments in a 1×1 box gave $A = 2.8$, $\gamma = 0.96$, and $\beta = 0.29$ [9]. The discrepancy with theory may be due to the fact that the small aspect ratio box imposes artificial constraints on the flow affecting the scaling relationship. It was also observed that high Rayleigh number solutions became time-dependent. Forced steady state simulations in a 4×1 box [6] give $A = 2.1$, $\gamma = 1.33$, and $\beta = 0.33$ [7] in approximate agreement with flat lid boundary layer theory [9]. For time-dependent convection, it is found numerically [6,7] that $\zeta = 1 + \beta$ and $\beta = n/(n + 2)$ in good agreement with viscous dissipation scaling theory and boundary layer stability analysis [8]. An extensive summary of scaling relationship parameters for both steady-state and time-dependent convection determined by various studies can be found in [7].

2. Equations of convection

2.1. Hydrodynamic equations

In the Boussinesq approximation, the hydrodynamic equations describing Rayleigh Benard convection in two dimensions are:

$$\begin{aligned} \frac{\partial u_i}{\partial x_i} &= 0, \\ \rho \left(\frac{\partial u_i}{\partial t} + u_j \frac{\partial u_i}{\partial x_j} \right) &= -\frac{\partial p}{\partial x_i} + \frac{\partial}{\partial x_j} \eta \frac{\partial u_i}{\partial x_j} + \rho g \alpha T \delta_{i2}, \\ \frac{\partial T}{\partial t} + u_j \frac{\partial T}{\partial x_j} &= \kappa \frac{\partial}{\partial x_j} \frac{\partial T}{\partial x_j}, \end{aligned} \quad (5)$$

where $x_i = (x, z)$ are the horizontal and vertical coordinates, u_i is velocity, p is deviatoric pressure, T is temperature, and η is the viscosity. The coordinate origin is taken to be on the lower boundary, i.e. z increasing upward. To simplify the analysis we consider rigid boundaries. The boundary conditions are:

$$\begin{aligned} u_i &= 0, \quad z = 0, d, \\ T &= T_0, \quad z = 0, \\ T &= T_1, \quad z = d, \end{aligned} \quad (6)$$

where $T_0 - T_1 = \Delta T$ is the temperature difference across the layer.

2.2. Scaling analysis

The basic features of non-Newtonian stagnant lid convection are similar to those of Newtonian stagnant lid convection [8]. A linear temperature distribution in the lid results in an exponential growth of the

viscosity when approaching the surface. As a result, convection only penetrates into the cold lid a small distance

$$\delta \sim \frac{\delta_0}{\theta}, \quad (7)$$

where δ_0 is the lid thickness. The temperature drop across this thin rheological sublayer is

$$\Delta T_{\text{rh}} \sim \frac{\Delta T}{\theta}. \quad (8)$$

Balancing rheological sublayer buoyancy with a shear stress of the same order as the interior shear stress gives,

$$u_i \sim \frac{\kappa}{d} \left(\frac{Ra}{\theta} \right)^n \left(\frac{\delta}{d} \right)^{2n}. \quad (9)$$

On the other hand,

$$u_{\text{rh}} \sim \frac{\kappa d}{\delta^2}, \quad (10)$$

implying

$$u_i \sim \frac{\kappa}{d} \left(\frac{\delta}{d} \right)^{-3}. \quad (11)$$

Eliminating δ gives the interior velocity scale

$$u_i \sim \frac{\kappa}{d} \left(\frac{Ra}{\theta} \right)^{3n/(2n+3)}. \quad (12)$$

2.3. Non-dimensionalization

According to the previous section, the appropriate interior scales are

$$\begin{aligned} z \sim d, \quad t \sim \frac{d^2}{\kappa} \left(\frac{Ra}{\theta} \right)^{-3n/(2n+3)}, \quad u \sim \frac{\kappa}{d} \left(\frac{Ra}{\theta} \right)^{3n/(2n+3)}, \\ T - T_0 \sim \frac{\Delta T}{\theta}, \quad \eta \sim \frac{b^{1/n} e^{-\gamma T_i/n}}{(u/d)^{(n-1)/n}}, \quad p \sim \frac{b^{1/n} e^{-\gamma T_i/n}}{(u/d)^{-1/n}}. \end{aligned} \quad (13)$$

The non-dimensionalized hydrodynamic Eq. (5) are then [2]:

$$\begin{aligned} \frac{\partial u_i}{\partial x_i} &= 0, \\ \frac{1}{Pr} \left(\frac{Ra}{\theta} \right)^{-3n/2(2n+3)} \left(\frac{\partial u_i}{\partial t} + u_j \frac{\partial u_i}{\partial x_j} \right) &= -\frac{\partial p}{\partial x_i} + \frac{\partial}{\partial x_j} \frac{\partial u_i}{\partial x_j} + \left(\frac{Ra}{\theta} \right)^{2n/(2n+3)} T \delta_{i2}, \\ \frac{\partial T}{\partial t} + u_j \frac{\partial T}{\partial x_j} &= \left(\frac{Ra}{\theta} \right)^{-3n/(2n+3)} \frac{\partial}{\partial x_j} \frac{\partial T}{\partial x_j}, \end{aligned} \quad (14)$$

subject to boundary conditions:

$$\begin{aligned} u_i &= 0, & z &= 0, 1, \\ T &= 0, & z &= 0, \\ T &= -\theta, & z &= 1. \end{aligned} \quad (15)$$

3. Mean field theory

3.1. Mean field equations

The calculation closely follows that of [12] with much of the notation being the same. Two fields are defined,

$$\psi_1 = -\left(\frac{\partial u_i}{\partial t}\right)^2, \quad \psi_2 = -\left(\frac{\partial T}{\partial t}\right)^2, \quad (16)$$

which are zero in the steady state. When the state (u_i, T) is close to a steady state (u_{0i}, T_0) , then to first order in $u_i - u_{0i}$ and $T - T_0$,

$$\int \mathbf{d}\mathbf{x} \psi_1 = \frac{\partial \phi_1}{\partial t}, \quad \int \mathbf{d}\mathbf{x} \psi_2 = \frac{\partial \phi_2}{\partial t}, \quad (17)$$

where

$$\begin{aligned} \phi_1 &= \int \mathbf{d}\mathbf{x} \left[\frac{1}{2} \left(\frac{Ra}{\theta}\right)^{-3n/(2n+3)} Pr \left(\frac{\partial u_i}{\partial x_j}\right)^2 - u_{0i} u_{0j} \frac{\partial u_i}{\partial x_j} - Pr \left(\frac{Ra}{\theta}\right)^{-n/(2n+3)} T_0 u_2 \right], \\ \phi_2 &= \int \mathbf{d}\mathbf{x} \left[\frac{1}{2} \left(\frac{Ra}{\theta}\right)^{-3n/(2n+3)} \left(\frac{\partial T}{\partial x_j}\right)^2 - u_{0j} T_0 \frac{\partial T}{\partial x_j} \right]. \end{aligned} \quad (18)$$

If, to first order, $u_i = u_{0i} + \delta u_i$, $T = T_0 + \delta T$, $\phi_1 = \phi_{10} + \delta \phi_1$ and $\phi_2 = \phi_{20} + \delta \phi_2$, then because ϕ_1 and ϕ_2 are constant in time for the steady state, $\delta \phi_1$ and $\delta \phi_2$ must vanish for all δu_i and δT . In other words, the equations:

$$\left(\frac{\delta \phi_1}{\delta u_i}\right)\Big|_0 = \left(\frac{\delta \phi_2}{\delta T}\right)\Big|_0 = 0, \quad (19)$$

where the expressions are evaluated at the steady state, reduce to the steady state form of the original hydrodynamic Eq. (5). Consider a pattern of convection such that

$$u_{x,z} = \left(\frac{DW}{a^2} \frac{\partial f}{\partial x}, Wf\right), \quad (20)$$

and

$$T = T_0 + Ff, \quad (21)$$

where $D = d/dz$, W , T_0 and F are arbitrary functions of z and t , and f is a periodic function of x satisfying

$$\frac{\partial^2 f}{\partial x^2} = -a^2 f, \quad (22)$$

normalized such that $\langle f^2 \rangle = 1$ (brackets denote horizontal average) where a is the wavenumber of the convection pattern. For the purposes of this work, we also choose $\langle f \rangle = \langle f^3 \rangle = 0$. Substituting (20) and (21) in (18) and integrating over x yields,

$$\phi_1 = Pr \left(\frac{Ra}{\theta} \right)^{-3n/(2n+3)} \int dz \left\{ \frac{1}{2} \left[2(DW)^2 + \frac{1}{a^2} (D^2 W)^2 + a^2 W^2 \right] - \left(\frac{Ra}{\theta} \right)^{2n/(2n+3)} F_0 W \right\}, \quad (23)$$

$$\phi_2 = \int dz \left\{ \frac{1}{2} \left(\frac{Ra}{\theta} \right)^{-3n/(2n+3)} \left[a^2 F^2 + (DT_0)^2 + (DF)^2 \right] - T_{00} D(FW_0) - F_0 W_0 DT_0 \right\}.$$

Noting that δT and δu_i satisfy the boundary conditions, it follows that

$$\delta\phi_1 = a^2 Pr \left(\frac{Ra}{\theta} \right)^{-3n/(2n+3)} \int dz \delta W \left\{ (D^2 - a^2)^2 W - a^2 \left(\frac{Ra}{\theta} \right)^{2n/(2n+3)} F_0 \right\}, \quad (24)$$

$$\delta\phi_2 = - \int dz \left\{ \delta T_0 \left[\left(\frac{Ra}{\theta} \right)^{-3n/(2n+3)} D^2 T_0 - D(F_0 W_0) \right] + \delta F \left[\left(\frac{Ra}{\theta} \right)^{-3n/(2n+3)} (D^2 - a^2) F - W_0 DT_{00} \right] \right\}.$$

Thus,

$$\begin{aligned} & \frac{1}{a^2 Pr} \left(\frac{Ra}{\theta} \right)^{3n/(2n+3)} \frac{\delta\phi_1}{\delta W} \\ &= (D^2 - a^2)^2 W - a^2 \left(\frac{Ra}{\theta} \right)^{2n/(2n+3)} F_0 - \frac{\delta\phi_2}{\delta T_0} = \left(\frac{Ra}{\theta} \right)^{-3n/(2n+3)} D^2 T_0 - D(F_0 W_0) - \frac{\delta\phi_2}{\delta F} \\ &= \left(\frac{Ra}{\theta} \right)^{-3n/(2n+3)} (D^2 - a^2) F - W_0 DT_{00}. \end{aligned} \quad (25)$$

The left hand sides vanish in the steady state $W = W_0$, $T_0 = T_{00}$ and $F = F_0$. Thus, dropping the subscript, the equations of steady convection in the actively convecting interior are

$$\left(\frac{Ra}{\theta} \right)^{-3n/(2n+3)} D^2 T_0 = D(FW), \quad (26)$$

$$\left(\frac{Ra}{\theta} \right)^{-3n/(2n+3)} (D^2 - a^2) F = WDT_0, \quad (27)$$

$$(D^2 - a^2)^2 W = a^2 \left(\frac{Ra}{\theta} \right)^{2n/(2n+3)} F, \quad (28)$$

subject to

$$\begin{aligned} W = DW = F = 0, & \quad z = 0, 1, \\ T_0 = 0, & \quad z = 0, \\ T_0 = -\theta, & \quad z = 1. \end{aligned} \quad (29)$$

Integrating (26)

$$DT_0 = \left(\frac{Ra}{\theta}\right)^{3n/(2n+3)} FW - Nu\theta, \quad (30)$$

where in the steady state, $Nu = -\theta^{-1}DT_0|_{0,1}$. Integrating (30) over the actively convecting layer and eliminating F using (28),

$$\theta Nu \sim 1 + a^{-2} \left(\frac{Ra}{\theta}\right)^{n/(2n+3)} \int_0^1 W(D^2 - a^2)W dz. \quad (31)$$

Eliminating F and T_0 from (27) using (28) and (30),

$$\delta_p^4 (D^2 - a^2)^3 W = W \left[W(D^2 - a^2)^2 W - a^2 Nu \theta \left(\frac{Ra}{\theta}\right)^{-n/(2n+3)} \right]. \quad (32)$$

Finally, eliminating Nu from (31) using (32),

$$\int_0^1 \frac{1}{W} (D^2 - a^2)^3 W \sim -a^2 \left(\frac{Ra}{\theta}\right)^{5n/(2n+3)}. \quad (33)$$

3.2. Boundary layer analysis

In the boundary layer limit [13], $Ra \rightarrow \infty$, (32) implies

$$W(D^2 - a^2)^2 W = a^2 Nu \theta \left(\frac{Ra}{\theta}\right)^{-n/(2n+3)}, \quad (34)$$

for the mainstream. If $aW < DW$ as $z \rightarrow 1 - \delta_0$, then the solution of (34) which satisfies $W = DW = 0$ at the bottom of the lid is

$$W \sim \left(a^2 Nu \theta \left(\frac{Ra}{\theta}\right)^{-n/(2n+3)} \right)^{1/2} (1 - \delta_0 - z)^2 \left[\ln \left(\frac{1}{1 - \delta_0 - z} \right) \right]^{1/2}. \quad (35)$$

Introducing a rheological boundary layer variable at $z = 1 - \delta_0$,

$$\eta = \frac{1 - \delta_0 - z}{\delta}, \quad \frac{d}{dz} = -\frac{1}{\delta} \frac{d}{d\eta}, \quad (36)$$

implies

$$W \sim \left(a^2 Nu \theta \left(\frac{Ra}{\theta}\right)^{-n/(2n+3)} \right)^{1/2} \delta^2 \left[\ln \left(\frac{1}{\delta} \right) \right]^{1/2} \left[\eta^2 - \frac{\eta^2 \log \eta}{2 \log(1/\delta)} + \dots \right], \quad (37)$$

with higher order log–log terms. On the other hand, in the mainstream, $D \sim 1$ and if a is large, the interior velocity scale,

$$W \sim \left(\frac{Nu\theta}{a^2} \left(\frac{Ra}{\theta} \right)^{-n/(2n+3)} \right)^{1/2}. \quad (38)$$

Thus, matching the interior solution to (35) requires a layer beneath the rheological boundary layer where $D \sim a$.

From (37), the contribution from the boundary layer to the integral in (33) is

$$\delta^{-5} \left[\log \left(\frac{1}{\delta} \right) \right]^{-1}.$$

In the layer where $D \sim a$, the contribution to the integral is $\sim a^5$ which is negligible compared to the boundary layer contribution as it was assumed that $aW < DW \sim W/\delta$ in the boundary layer. In the remainder of the interior flow, $D \sim 1$ and the contribution to the integral is $-a^6$. Thus, (33) becomes,

$$\frac{1}{\delta^5 \log(1/\delta)} + a^6 \sim a^2 \frac{Ra}{\theta} \delta^{5n/(2n+3)}. \quad (39)$$

If

$$a \sim \left(\frac{Ra}{\theta} \right)^{5n/4(2n+3)}, \quad (40)$$

then

$$\delta \sim \left(\frac{Ra}{\theta} \right)^{-3n/2(2n+3)} \left[\log \left(\frac{Ra}{\theta} \right) \right]^{-1/5}. \quad (41)$$

Substituting W in (32),

$$Nu \sim a^{-2} Ra^{-1} \left(\frac{Ra}{\theta} \right)^{-3(n-1)/(2n+3)} \delta^{-6} \left[\log \left(\frac{1}{\delta} \right) \right]^{-1}. \quad (42)$$

Finally, substituting for δ and a yields the Nusselt number scaling relationship,

$$Nu \sim \theta^{-1} \left(\frac{Ra}{\theta} \right)^{3n/2(2n+3)} \left[\log \left(\frac{Ra}{\theta} \right) \right]^{1/5}. \quad (43)$$

4. Numerical experiments

Stagnant lid, convective heat transfer was studied in a large aspect ratio box [6] for a viscosity law of the form,

$$\eta = \frac{b}{\tau^{n-1}} \exp(-\gamma_T T + \gamma_z z). \quad (44)$$

Based on systematic numerical experiments the authors identified a low Rayleigh number, steady state regime characterized by large scale, stationary convection [1,2,9] and a high Rayleigh number,

time-dependent regime characterized by development of convective instabilities at the base of the lid [8]. A direct comparison with mean field theory can be made for the purely temperature-dependent viscosity cases ($\gamma_z = 0$).

In the time-dependent case, the data can be fit with a scaling relationship suggested by stability analysis [8,7],

$$Nu = (0.31 + 0.22n)\theta^{-2(n+1)/(n+2)} Ra_i^{n/(n+2)}, \tag{45}$$

where Ra_i is defined in terms of the temperature at the lid base. For the mean field theory, a one-parameter fit for the scaling coefficient gives,

$$Nu = (0.16 + 0.43n)\theta^{-(7n+6)/(2(2n+3))} Ra_i^{3n/(2(2n+3))} \left[\log \left(\frac{Ra_i}{\theta} \right) \right]^{1/5}. \tag{46}$$

These results are compared in Fig. 1. The Nusselt number rms misfits are 0.36 and 0.44 ($n = 1$) and 0.33 and 0.13 ($n = 3$) for (47) and (48), respectively.

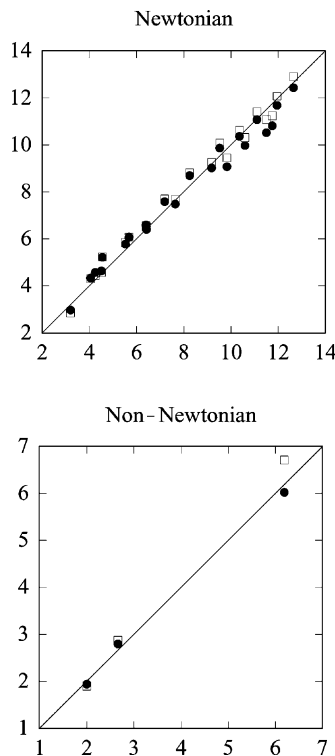


Fig. 1. The time-dependent Nusselt number calculated using the fitting formula (model) vs. the numerical data (data) for Newtonian viscosity. Open squares correspond to boundary layer stability analysis (47) and black circles to the mean field result for the wavenumber that maximizes the heat transfer (48).

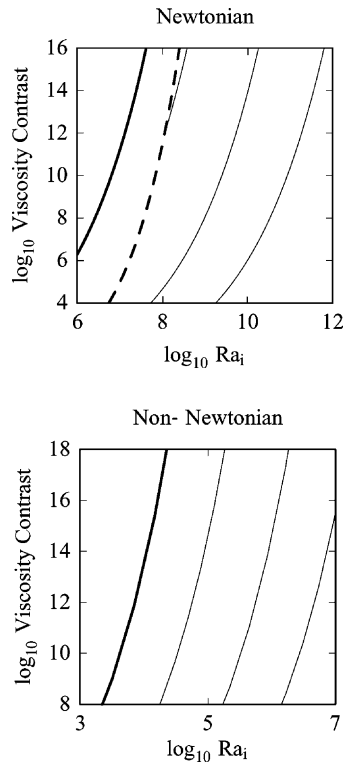


Fig. 2. Stagnant lid convection Nusselt number contours in Ra_i - θ space. The thin solid lines are $Nu = [3, 10, 30]$ contours. The thick solid line is the stability curve [8]. For Newtonian viscosity, the thick dashed line is the location of the transition to time-dependent convection [6]. For non-Newtonian viscosity, steady convection occurs only in a narrow parameter range and the transition to time-dependence is not well constrained.

5. Discussion and conclusions

The results are summarized in Fig. 2 which shows Nusselt number contours in terms of the interior Rayleigh number and viscosity contrast. In both cases, the thick solid line is approximately the stagnant lid convection stability curve [8]. In the Newtonian case, the thick dashed line indicates the approximate location of the transition to time-dependent convection [6]. In the non-Newtonian case, this transition is not well constrained.

It should be mentioned that while the analysis presented here strictly applies to convection rolls, squares, or rectangles, the method is generalizable to other planforms [12]. Data for stagnant lid convective heat transfer in three-dimensional Cartesian boxes is limited [11]. Whether free slip or mixed boundary conditions can be analyzed requires further study. However, stagnant lid heat transfer is insensitive to the upper boundary condition and the lower boundary condition can only change the coefficient in the Nu - Ra relationship but not the scaling exponents.

The results are most applicable to low Rayleigh number, pseudo-steady state convection (Fig. 1). Although the mean field Nu - Ra relationship approximately fits the higher Rayleigh number data, convection in this regime is characterized by different dynamics [7]. Whether this has some physical meaning or

is just a coincidence is an open question. More data may help to answer this question. This situation is similar to the Newtonian, constant viscosity case where [14] note an excellent fit of the mean field result [12,13] to experimental data on heat transport by turbulent convection of cryogenic helium gas over a wide range of Rayleigh numbers [15]. It should also be mentioned that studies of constant viscosity mean field convection suggest that single a solution are unstable at high Rayleigh numbers and that multiple a solution are preferred [16].

References

- [1] S. Morris, D. Canright, A boundary layer analysis of Benard convection in a fluid of strongly temperature dependent viscosity, *Phys. Earth Planet. Int.* 36 (1984) 355–373.
- [2] A.C. Fowler, Fast thermoviscous convection, *Stud. Appl. Math.* 72 (1985) 1–34.
- [3] A. Davaille, C. Jaupart, Transient high Rayleigh number thermal convection with large viscosity variations, *J. Fluid Mech.* 253 (1993) 141–166.
- [4] L.-N. Moresi, V.S. Solomatov, Numerical investigations of 2D convection with extremely large viscosity variations, *Phys. Fluids* 7 (1995) 2154–2162.
- [5] V.S. Solomatov, L.-N. Moresi, Three regimes of mantle convection with non-Newtonian viscosity and stagnant lid convection on the terrestrial planets, *Geophys. Res. Lett.* 24 (1997) 1907–1910.
- [6] C. Dumuloin, M.P. Doin, L. Fleitout, Heat transport in stagnant lid convection with temperature and pressure dependent Newtonian or non-Newtonian rheology, *J. Geophys. Res.* 104 (1999) 12759–12777.
- [7] V.S. Solomatov, L.-N. Moresi, Scaling of time dependent stagnant lid convection: application to small scale convection on Earth and other terrestrial planets, *J. Geophys. Res.* 105 (2000) 21795–21817.
- [8] V.S. Solomatov, Scaling of temperature and stress dependent viscosity convection, *Phys. Fluids* 7 (1995) 266–274.
- [9] C.C. Reese, V.S. Solomatov, L.-N. Moresi, Heat transport efficiency for stagnant lid convection with dislocation viscosity: applications to Mars and Venus, *J. Geophys. Res.* 103 (1998) 13643–13658.
- [10] O. Grasset, E.M. Parmentier, Thermal convection in a volumetrically heated, infinite Prandtl number fluid with strongly temperature dependent viscosity: implications for planetary evolution, *J. Geophys. Res.* 103 (1998) 18171–18181.
- [11] R.A. Trompert, U. Hansen, On the Rayleigh number dependence of convection with a strongly temperature dependent viscosity, *Phys. Fluids* 10 (1998) 351–360.
- [12] P.H. Roberts, in: R. Donnelly, R. Herman, I. Prigogine (Eds.), *Non-Equilibrium Thermodynamics, Variational Techniques, and Stability*, University of Chicago Press, Chicago, 1966, pp. 125–162.
- [13] K. Stewartson, in: R. Donnelly, R. Herman, I. Prigogine (Eds.), *Non-Equilibrium Thermodynamics, Variational Techniques, and Stability*, University of Chicago Press, Chicago, 1966, pp. 158–162.
- [14] J.J. Niemela, L. Skrbek, K.R. Sreenivasan, R.J. Donnelly, Turbulent convection at very high Rayleigh numbers, *Nature* 404 (2000) 837–840.
- [15] L.P. Kadanoff, Turbulent heat flow: structures and scaling, *Phys. Today* 54 (2001) 34–39.
- [16] S.-K. Chan, Infinite Prandtl number turbulent convection, *Stud. Appl. Math.* 50 (1971) 13–49.